

# VPLIV ZAobljenosti DELCEV IN MORFOLOGIJE NA STRIŽNI PORUŠNI MEHANI- ZEM ZRNATIH ZEMLJIN POD PASOVNIMI TEMELJI

**Babak Karimi Ghalehjough** (vodilni avtor)  
Ataturk University,  
Department of Civil Engineering  
No.318, Ataturk University, 25240 Erzurum, Turčija  
E-pošta: karimi.babak@gmail.com

**Suat Akbulut**  
Yildiz Technical University,  
Department of Civil Engineering  
34220 Esenler, İstanbul, Turčija  
E-pošta: sakbulut@yildiz.edu.tr

**Semet Çelik**  
Ataturk University,  
Department of Civil Engineering  
No.318, Ataturk University, 25240 Erzurum, Turčija  
E-pošta: scelik@atauni.edu.tr

## Izvleček

V članku je raziskovan učinek zaobljenosti delcev in morfologije na strižni porušni mehanizem zrnate zemljine. Pasovni temelj je bil modeliran v laboratorijskih pogojih. Apnenčasta zemljina je bila preizkušena s tremi razredi zaobljenosti zrn: koničasta, zaobljena in dobro zaobljena zrna z velikostmi od 0,30 mm do 4,75 mm. Ti so bili razdeljeni v šest različnih skupin pri treh relativnih gostotah 30 %, 50 % in 70 %. Da bi razumeli mehanizem deformacije zrnate zemljine je bila med preizkusi narejena vrsta fotografij in izvedena analiza z metodo slik sledilnih delcev (PIV). Rezultati so pokazali, da je povečanje velikosti vzorcev povečalo prizadeto območje zemljine. Hkrati pa je povečanje relativne gostote povzročilo prehodni porušitveni mehanizem, ki je prešel proti splošni porušitvi. Mehanizem strižne porušitve zemljine se je spremenil iz splošnega v prehodni porušitveni mehanizem z večanjem zaobljenosti delcev. Ta učinek je bil večji pri manjših drobnejših materialih. Vplivno območje je segalo globlje pri vzorcih s koničastimi zrnami kot pri vzorcih z zaobljenimi in dobro zaobljenimi zrnami. Ugotovljena globina v zemljini s koničastimi zrnami je bila približno 1,5B v najmanjši velikostni skupini medtem, ko je bila več kot 3B in blizu 4B v skupini z največjo velikostjo zrn. V zemljinah s koničastimi zrnami je treba upoštevati stranske sloje in spodnje sloje zemljin. Območje pod temelji postane pomembnejše od stranskih delov s povečanjem zaobljenosti delcev.

## Ključne besede

zaobljenost zrn, morfologija delcev, strižni porušni mehanizem, pasovni temelj, metoda s sliko sledilnih delcev PIV, mejna nosilnost

# EFFECT OF PARTICLE ROUNDNESS AND MORPHOLOGY ON THE SHEAR FAILURE MECHANISM OF GRANULAR SOIL UNDER STRIP FOOTING

**Babak Karimi Ghalehjough** (corresponding author)

Ataturk University,  
Department of Civil Engineering  
No.318, Ataturk University, 25240 Erzurum, Turkey  
E-mail: karimi.babak@gmail.com

**Suat Akbulut**

Yildiz Technical University,  
Department of Civil Engineering  
34220 Esenler, İstanbul, Turkey  
E-mail: sakbulut@yildiz.edu.tr

**Semet Çelik**

Ataturk University,  
Department of Civil Engineering  
No.318, Ataturk University, 25240 Erzurum, Turkey  
E-mail: scelik@atauni.edu.tr

## Keywords

particle roundness, morphology of particles, shear failure mechanism, strip footing, PIV method, ultimate bearing capacity

**DOI** <https://doi.org/10.18690/actageotechslov.15.1.43-53.2018>

## Abstract

*This study investigates the effect of particles roundness and morphology on the shear failure mechanism of soil. A strip footing was modeled under laboratory conditions. Calcareous soil was tested with three roundness classes: angular, rounded and well-rounded shapes with sizes of 0.30 mm to 4.75 mm. These were divided into six different groups at three relative densities of 30%, 50% and 70%. A series of photographs was taken during the tests and analyzed using the particle image velocimetry (PIV) method to understand the soil-deformation mechanism. The results showed that increasing the sample sizes increased the affected area of the soil. At the same time, increasing the relative density caused a punching failure mechanism that went towards the general failure. The shear failure mechanism of the soil changed from general toward punching shear failure with increasing particle roundness. This effect was larger with the smaller materials. Underneath the affected layers of soil, the angular samples were deeper than the rounded and well-rounded samples. The affected depth in the angular soil was approximately 1.5B in the smallest size group. This was more than 3B and near 4B in the largest size group. Both the sides and the underlying soil layers should be considered on angular soils. The area under the footing becomes more important than the side parts after increasing the roundness of the particles.*

## 1 INTRODUCTION

Soil's geotechnical properties primarily affect its behavior. One of these properties is particle shape. The texture, sphericity, roundness and roughness are used to describe the particle shapes [1, 2]. Holtz and Gibbs [3] showed that the shear strength of angular materials is more than the rounded or well-rounded materials. Other studies showed that by increasing the angularity of the materials, the maximum and minimum void ratios ( $e_{max}$  and  $e_{min}$ ) decreased [2, 4, 5]. There are many studies on size or particle shape and their effect on the behavior of aggregates under loading. Direct shear box tests have been made on samples prepared with groups of natural river soil and crushed gravels and fine soil including clay and silt. Yanrong studied the effect of size distribution and particle shape [6].

Arasan et al. [7] studied calcareous, ballast, abrasive and bearing balls. The shape properties of the particles were calculated by considering the roundness values, and the soils were divided into six roundness classes. Calcareous soil changed from angular to rounded and well-rounded, and the effect of the particle shapes on the geotechnical properties of the aggregate was studied.

The ultimate bearing capacity of the strip footing is one of the most important issues in civil engineering [8]. Many researches and investigations have been made on strip footing. Reinforcing the soil can improve the settlement of the footing or bearing capacity of the soil [9, 10, 11, 12, 13, 14]. Different kinds of soils such as gravel, sandy soil, clay and silt under different conditions in normal or reinforced soil have been studied. Previous researchers have studied different conditions and the effect of different factors such as the shape of the footing, soil properties, reinforcement, ground-water level, etc. on the manner of the strip footing [15, 16, 17, 18].

Chen and Abu-Farsakh [19] studied the strip footing and ultimate bearing capacity of the reinforced soil. They developed an analytical solution for estimating the ultimate bearing capacity. The results showed that relative density of reinforced soil and underlying un-reinforced soil affected punching shear failure. Kuranchie et al. [20] studied load-settlement behavior of strip footing laid on iron ore tailings. Cicek et al. [21] studied reinforcing soil and the effect of reinforcement length on the strip footing behavior by geogrids. Reinforcement length as well as the types and number of reinforcements were tested to determine whether they affect the optimum reinforcement.

The effect of the ultimate load has also been studied [22]. This study measured the strip footing near a sandy slope. The slope was loaded centrally and randomly. Ultimate bearing capacity decreased by increasing the amount of eccentricity, and percentage of this decrease increased

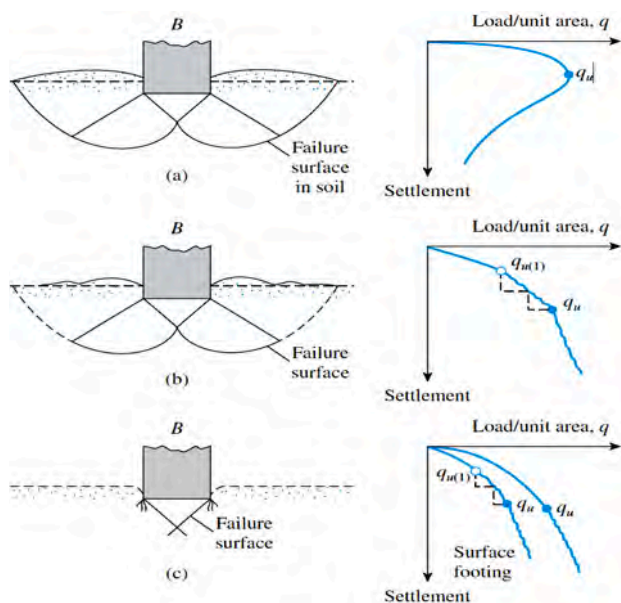


**Figure 1.** Failure mechanism of soil under shallow foundations: (a) general shear failure (b) local shear failure (c) punching shear failure [25, 26].

with increasing eccentricity. Depending on the soil's relative density, there are generally three shear-failure mechanisms under shallow foundations. Foundations on dense sand ( $Dr > 70\%$ ) fail with a mechanism marked by a peak resistance, which is known as general shear failure [23]. On sands with a relative density between 35% and 70% sudden failure is not realized. This type of failure is called local shear failure. Foundations placed on very loose sand with  $Dr < 35\%$  can penetrate into the soil with no bulging observed on the surface; this failure type is also called punching shear [24]. Soils with relative densities over 70% show a general shear failure mechanism under shallow foundations [25]. Fig.1 shows three shear-failure mechanisms for soil under shallow foundations. This figure shows that the punching mechanism of the soil moves downward directly below the foundation, but the local and general failure mechanisms can facilitate movement to the surface of the soil [25, 26].

The particle image velocimetry (PIV) method explains the sandy soil's movement. It measures the soil particle movement for the whole soil mass [27, 28]. Slominski [29] used PIV method to measure dry cohesion-free sand movement in silos. The surface deformation in silos was studied in laboratory model tests, and effect of the roughness of silo walls and sand density on the volumetric strain was reported. The accuracy of the measurements was discussed and advantages and disadvantages of the PIV method were outlined here. Ould Baba and Peth [30] studied the creep deformation of slopes with a large-scale soil box via PIV. The efficiency of the PIV method was examined, and effect of hydraulic stresses on the creep deformation was studied using model tests.

There are many studies that use strip footing or particle properties, but the effect of particle roundness and shape on the soil behavior and the failure mechanism of soil are missing from the literature. This study is novel because it measures the effect of particle shape and roundness on the soil behavior under strip footings. The failure mechanism of the aggregate was studied with the PIV method at different values of roundness, density, and size.

## 2 MATERIAL AND METHODS

### 2.1 Soil

The soil was calcareous and prepared by the Ergunler Company in Erzurum, Turkey. According to ASTM 854-14, [31] the soil's specific gravity was 2.7; soil was angular. After taking the soil to the laboratory, it was washed and dried by spreading on a dry surface at room temperature and then sieved to six different sizes

between 0.30 mm to 4.75 mm. Tests were made on the angular, rounded and well-rounded soils. The angular calcareous soil changed to sub-rounded and rounded calcareous. It can be changed to well-rounded calcareous soil via the Los Angeles Rattler machine. Here, angular soil was transformed in the Los Angeles machine without balls, as explained by Arasan [32, 39]. To change the angular calcareous soil to rounded soil, 50,000 revolutions were used. To change the angular soil to well-rounded calcareous soil, 100,000 revolutions were used on the Los Angeles machine. The roundness values

of the soils were determined using the Cox equation [33] and the Power [34] chart (Table 1).

According to the unified soil-classification system [35], soil samples were classified as poorly graded sand (SP). Grain size distribution increased according to ASTM-D 6913-04 [36], as shown in Fig. 2.

The roundness of the soil particles increased by going from angular soil towards rounded and well-rounded. It is even clear and easily visible by eye at larger sizes. Examples of the angular, rounded and well-rounded calcareous soils are shown in Fig. 3.

**Table 1.** Roundness properties of materials [7, 39].

Sample	Roundness Value	Roundness Class
Angular Calcareous	0.693-0.744	Angular - Sub Angular
Rounded Calcareous	0.786-0.803	Rounded - Well Rounded
Well-Rounded Calcareous	0.834-0.854	Well Rounded

### 2.2 Model Tank

This study involved a series of laboratory tests. The model tests were conducted in a model tank: 1 m × 0.1 m in plan and 1 m in depth. The tank was completely rigid to prevent any movement and the length of the model footing was almost equal to the width of the tank to maintain plain-strain conditions. The front side of

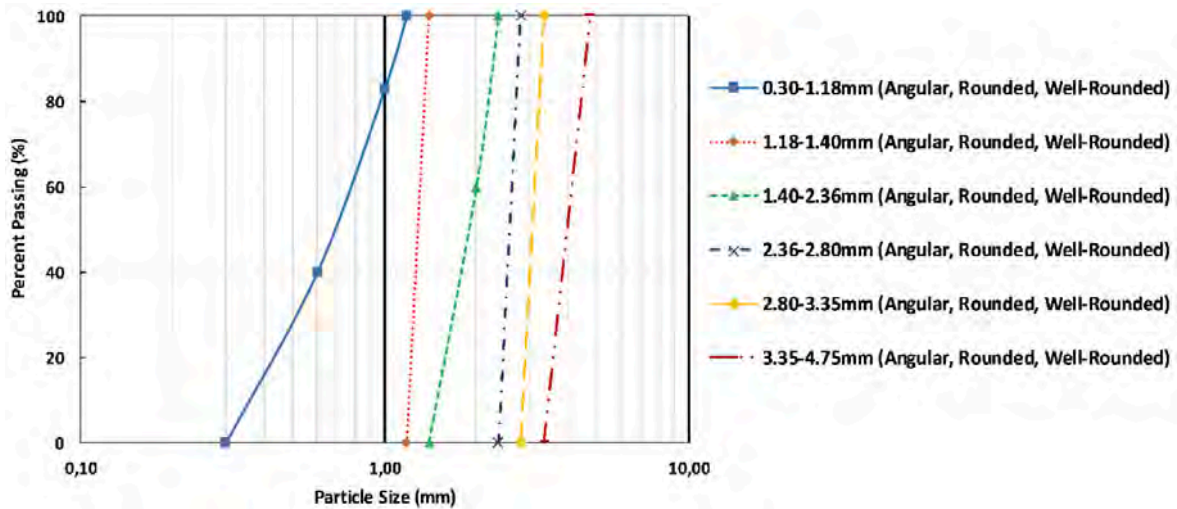


**Figure 2.** Grain size distributions of the soils.



**Figure 3.** Pictures of soil with three different roundness.

the tank was made of a sheet of Plexiglas to monitor and inspect the soil and model the footing and their movements during the tests. A polyamide strip footing was used: 9.8 cm long, 5 cm wide and 4 cm high. It was sufficiently rigid to prevent reshaping during tests. A hydraulic jack was fixed to a strong horizontal beam of the frame that could carry thrust developed by hydraulic jack without any deformation during tests. The speed of displacement was  $<2$  mm/min for applying loads over small increments. A 50-kN load cell was placed between the jack and footing to measure the applied load. The load was transferred to the footing via a shaft placed between the load cell and the footing. A ball bearing was placed between the shaft and the footing to apply a single point load to the footing. A rigid footing was used in this study, and a uniform load was applied from the footing to the soil. There was a 1-mm gap at each side of the tank to prevent contact between the side walls of the tank and the footing. Two sides of the footing and walls of the tank were coated with petroleum jelly to reduce the end-friction effects.

Two linear variable displacement transducers (LVDTs) were concurrently placed at the two corners of the model footing. The average movement of these two LVDTs was considered to be settlement of the footing.

Finally, the data from the load cell and the LVDTs were transferred to a computer via a data logger. To analyze the soil movement, a high-resolution digital camera was placed in front of the tank to take high-quality images. First, a picture was taken before starting the test without any movement in the soil or the footing. Images were acquired every 30 seconds until the end of the experiment. These pictures were used to analyze the

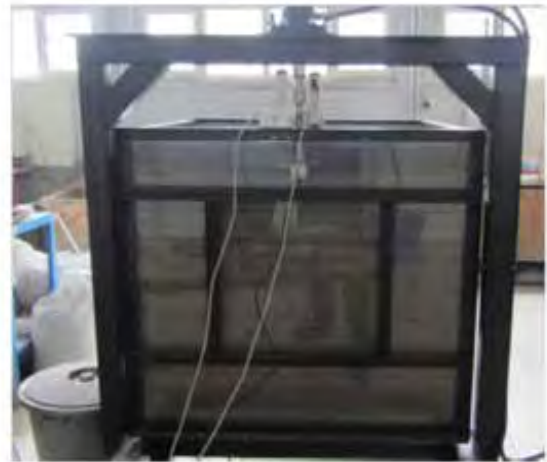


Figure 4. Pictures of the tank.

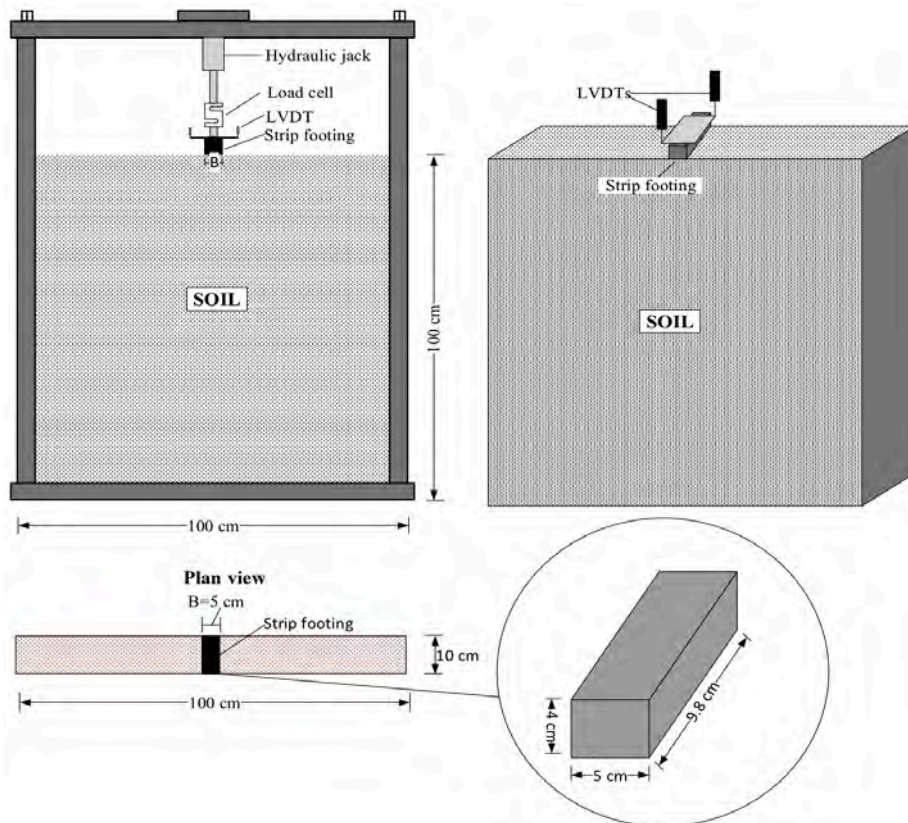


Figure 5. Schematic picture of the test box.

soil movement via the Geo-PIV program. Tank pictures and a schematic drawing of the model tank are shown in Figs. 4 and 5, respectively.

### 2.3 Experimental Setup

The soil was classified into six different sizes from 0.3 mm to 4.75 mm. There were three roundness classes: angular, rounded and well-rounded calcareous for each dimension. The tests were done at relative densities of 30%, 50% and 70% ( $Dr=30\%$ , 50% and 70%) for each group of dimensions and roundness classes. According to ASTM D4253-16 and ASTM D4254-16, [37, 38] the minimum and maximum void ratio ( $e_{min}$  and  $e_{max}$ ) of each soil sample was identified by considering the tank volume. The weight of the soil was calculated and placed in the tank at these three densities. There were 54 samples for testing, and each test was done at least in triplicate to ensure the results. Table 2 shows all the test conditions. After putting the soil inside the tank, a strip footing was placed on the soil surface, and two LVDTs at two cross corners of the footing were used to measure the settling of the model foundation.

**Table 2.** All 54 different conditions of the tests.

Soil Dimension (mm)	Relative Density (%)	Roundness Class
0.30–1.18	30 - 50 - 70	Angular, Rounded, Well-Rounded
1.18–1.40	30 - 50 - 70	Angular, Rounded, Well-Rounded
1.40–2.36	30 - 50 - 70	Angular, Rounded, Well-Rounded
2.36–2.80	30 - 50 - 70	Angular, Rounded, Well-Rounded
2.80–3.35	30 - 50 - 70	Angular, Rounded, Well-Rounded
3.35–4.75	30 - 50 - 70	Angular, Rounded, Well-Rounded

### 2.4 PIV Method

The Geo-PIV program can explain the mechanism of soil deformation under the footing. PIV is a velocity-measurement technique originally developed in the field of fluid mechanics. Soil deformation can be considered a low-velocity flow process [28]. This program is based on close-range photography and PIV. In Geo-PIV, digital photographs of planar soil deformation are studied with PIV to monitor the movement of the soil particles. To measure the soil movement, the program creates patches

on the pictures and compares each patch across the series of pictures. This shows the final movement of the particles for each patch as well as the whole soil [27]. Here, a digital camera is placed in front of the tank on a stable tripod to prevent any movement. The first picture was taken before starting the test. This explains the soil condition before adding any load. The second picture was taken 30 seconds after loading the footing, and then a series of pictures were taken every 30 seconds to the end of the test. All the pictures are high resolution, and there was no movement of the camera or the tank during the testing.

## 3 RESULTS AND DISCUSSIONS

The tests were made under laboratory conditions, and high-quality pictures were collected during the testing. Data from the load-cell and the LVDTs were transferred to the computer and a settlement-load graph was drawn for each test. These graphs show a failure point and a subsequent failure moment that is recognized for each test [24, 25]. Next, the pictures' step numbers were identified by considering the failure time. This series of pictures was analyzed with Geo-PIV software to understand the soil movement and the deformation from the beginning to the failure point. This was done for each test to evaluate the shear failure of the soil under the footing. Fig.6 shows the failure mechanism of the angular calcareous soils at six different dimensions and three different relative densities ( $Dr$ ; 30%, 50%, and 70%). The data suggest that the soil-failure mechanism goes from punching to general failure by increasing the relative density. The shear failure mechanism is punching at a 30% relative density. At  $Dr=50\%$ , this mechanism changed to local. By increasing the  $Dr$  to 70%, the soil-failure mechanism became a general shear failure.

The movement and deformation increase with the increasing soil size. The underlying layers of soil deform at dimensions of 0.30–1.18 mm near 1.5 B. At  $Dr=30\%$ , the 2B samples have a soil size of 3.35–4.75 mm at the same relative density. The side areas of the footing showed the same behavior on larger sizes. There is more area of soil under the footing. The inside soil was affected by the loading and even the soil mechanism went from punching to a general mechanism. By increasing the relative density of the soil, the influence of the aggregate size was more pronounced – especially on the side movements. More areas under the footing showed evidence of deformation. The deformation at larger sizes was more pronounced than with the finer soils.

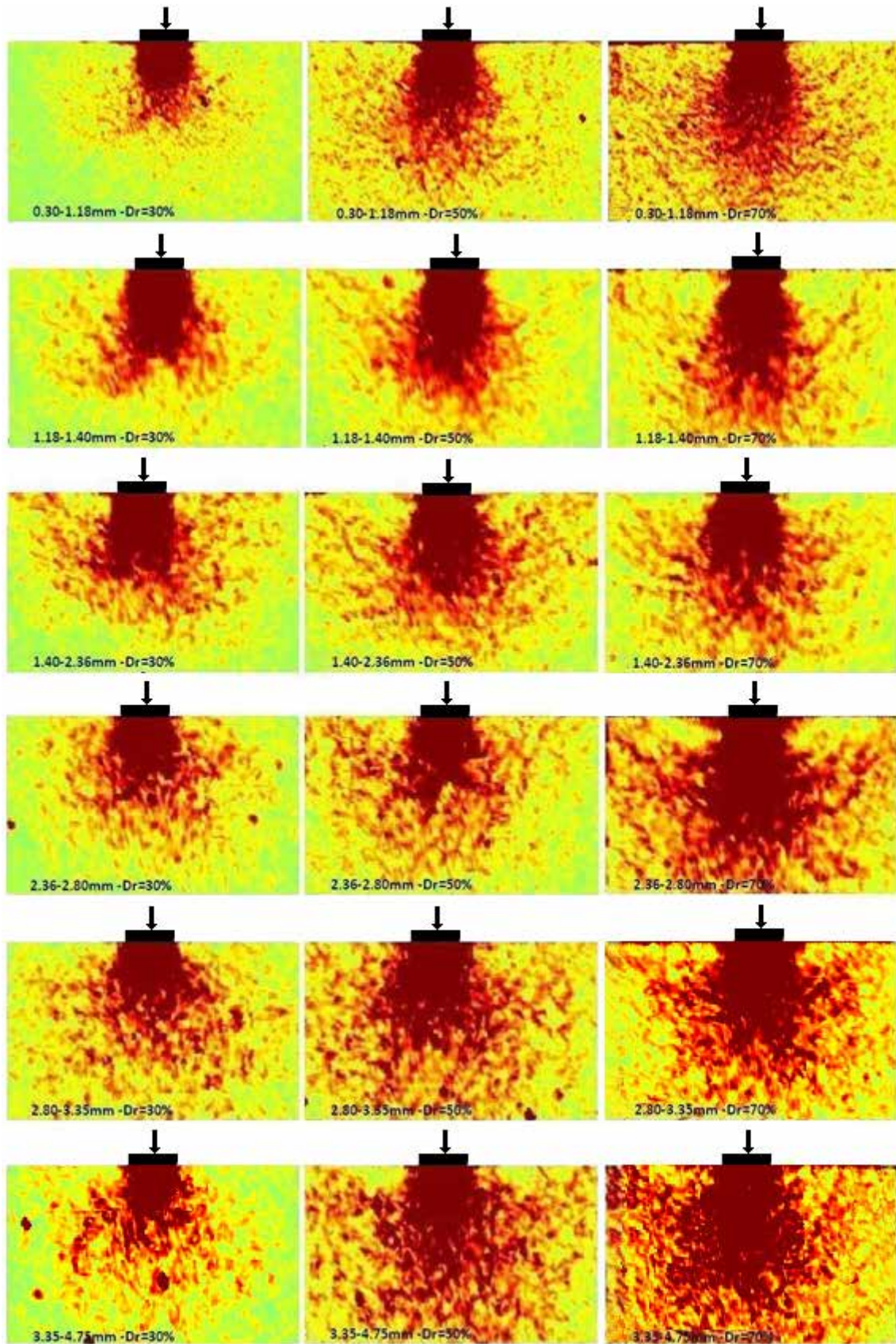


Figure 6. Failure mechanism of angular soil at different sizes and relative densities.

We also studied the effect of roundness on the soil-failure mechanism. The soil-failure mechanism was compared at three different relative densities and three roundness classes for all six dimensions. The soil movements under these conditions are seen in Fig.7 to 12. These mechanisms showed that by increasing the

roundness of the material there were decreases on the loading area under the footing. This was more visible for materials with dimensions of 0.30–1.18 than for those of 3.35–4.75 mm. This means that the effect of the roundness is more significant for finer materials than for larger materials.

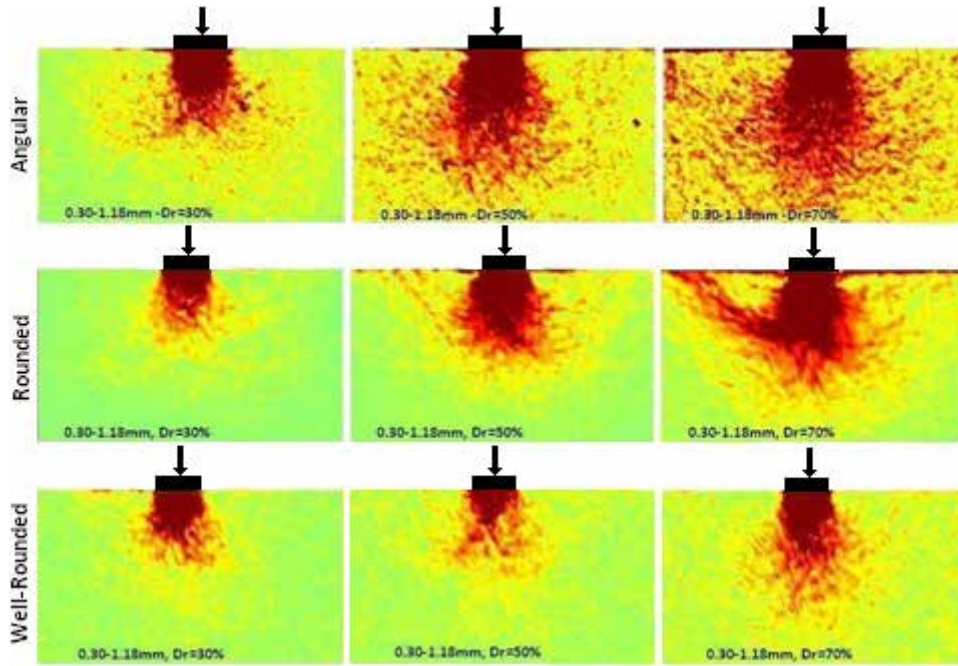


Figure 7. Failure mechanism of soils with dimensions of 0.30–1.18mm.

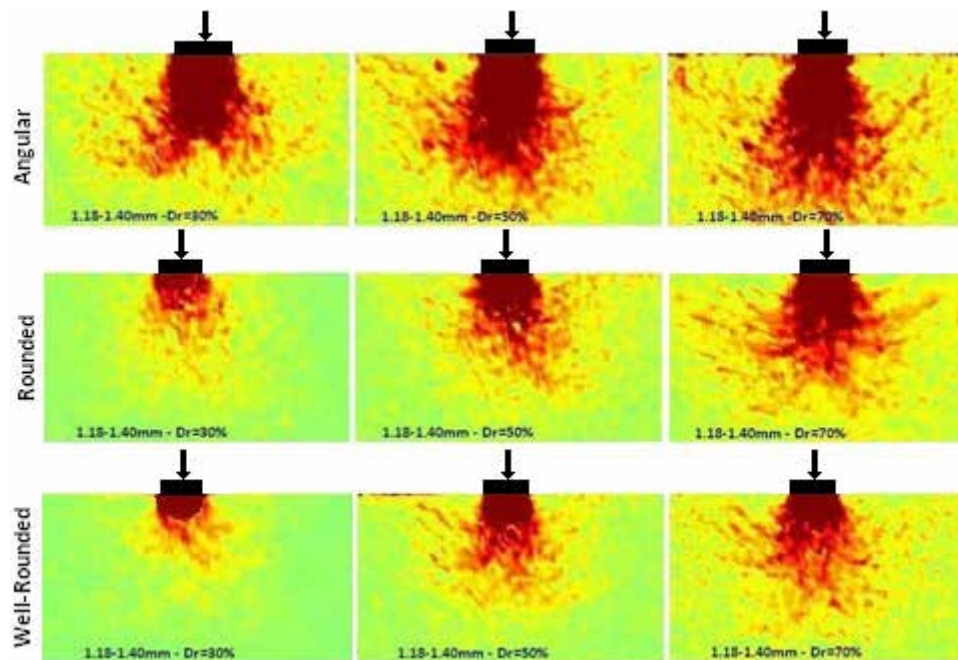


Figure 8. Failure mechanism of soils with dimensions of 1.18–1.40mm.

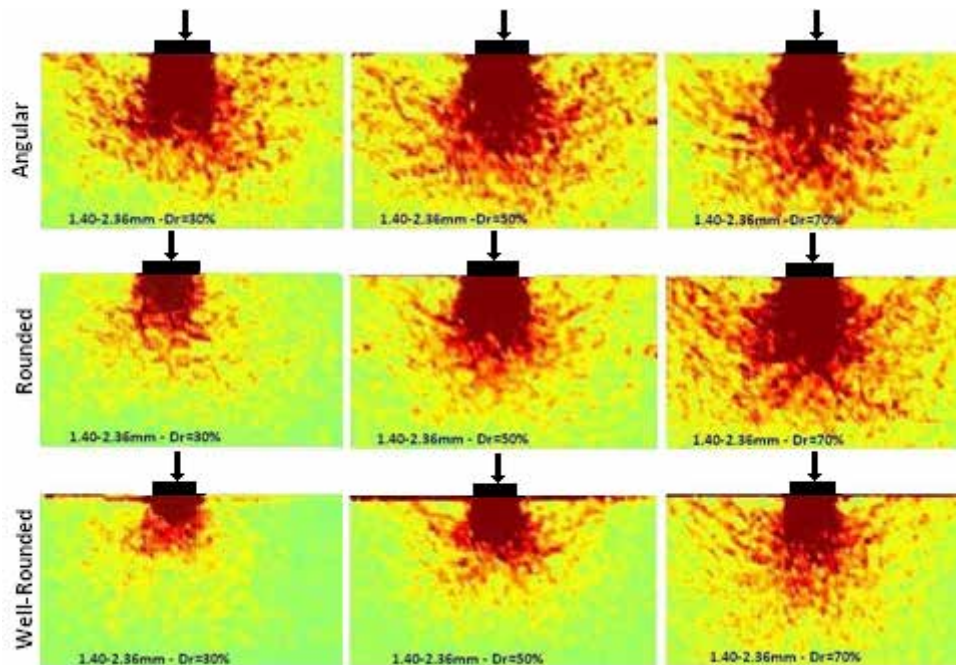


Figure 9. Failure mechanism of soils with dimensions of 1.40–2.36mm.

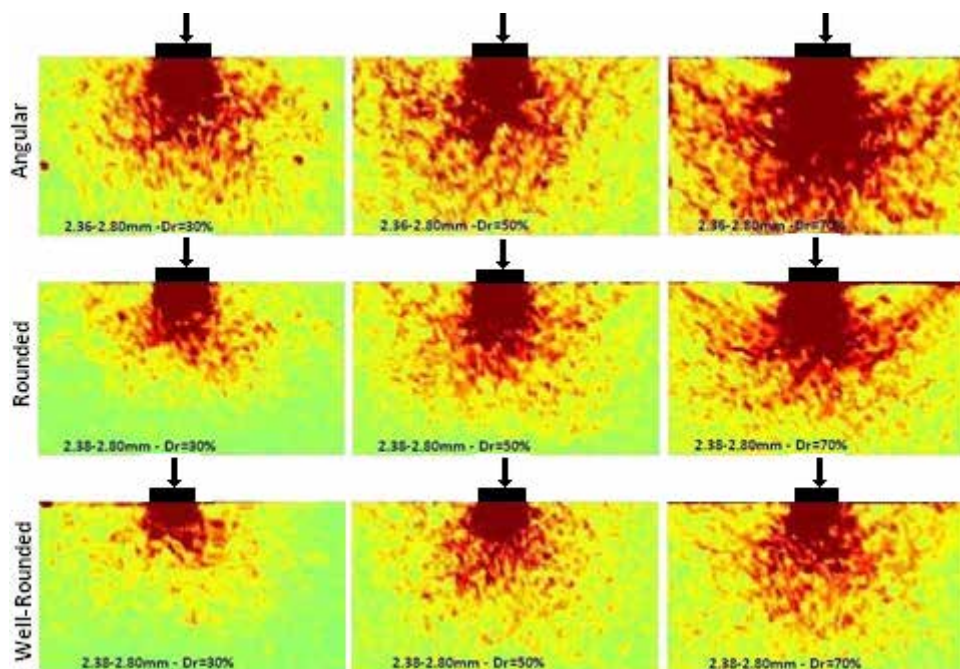


Figure 10. Failure mechanism of soils with dimensions of 2.36–2.80mm.

The soil behavior under three roundness conditions was different. Angular soils had punching failure at  $Dr=30\%$ , local shear failure at  $Dr=50\%$ , and general shear failure at  $Dr=70\%$ . However, the soil behavior under the footing changed by increasing the particle roundness. The movement of the well-rounded soil was between punching

and local at  $Dr=70\%$  with dimensions of 0.30–1.18 mm. Even at dimensions of 3.35–4.75 mm, well-rounded samples failed with a local shear failure mechanism at the same dimension and relative density. This is in contrast to the general failure mechanism of angular soil at a  $Dr$  of 70%.

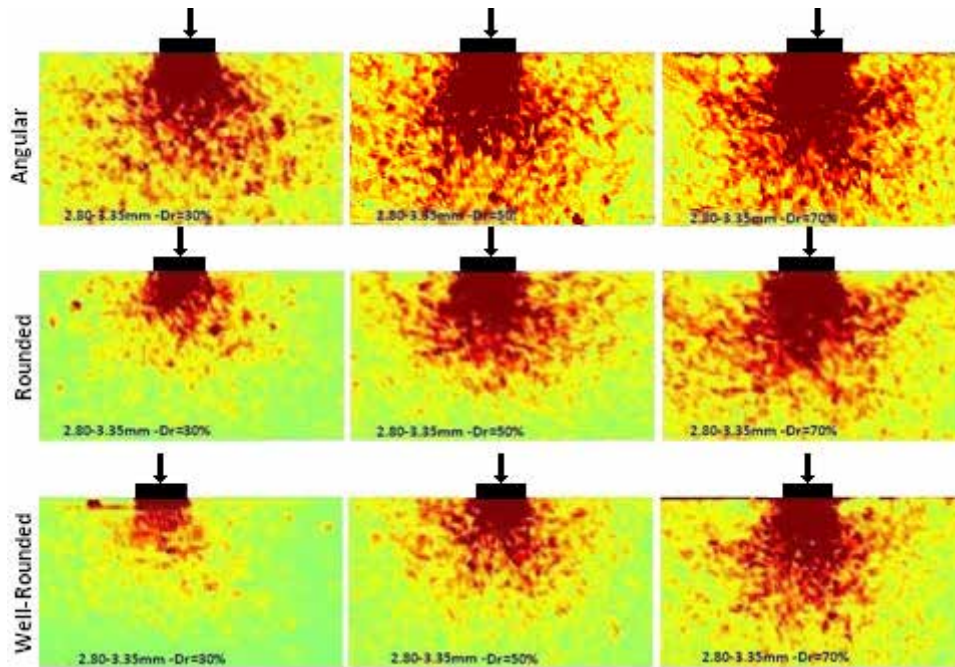


Figure 11. Failure mechanism of soils with dimensions of 2.80–3.35mm.

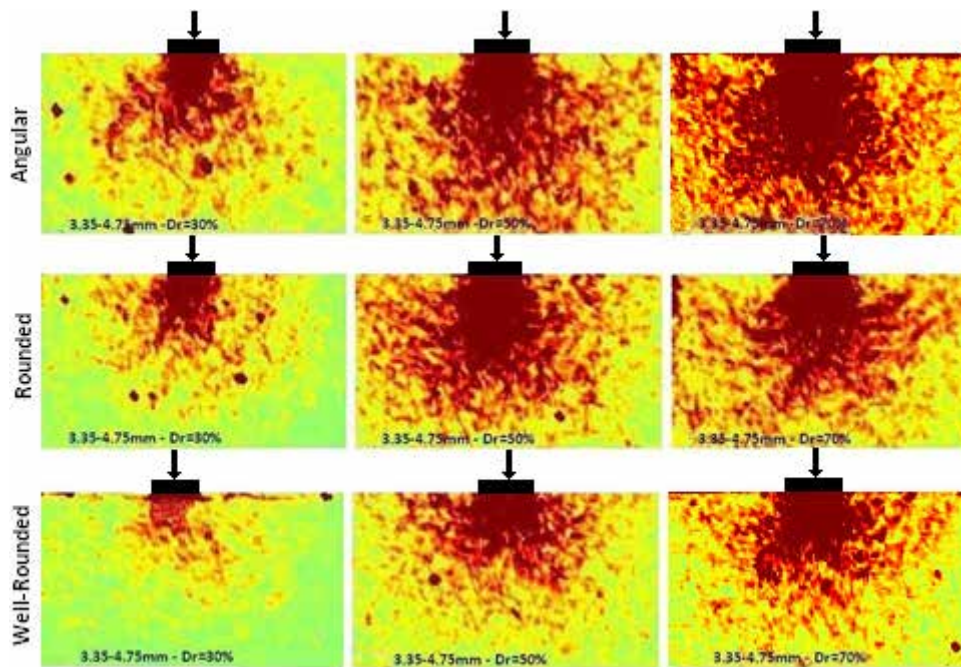


Figure 12. Failure mechanism of soils with dimensions of 3.35–4.75mm.

Particles can move on each other more easily in well-rounded soils than rounded or angular samples because of the shapes and roundness of the aggregates. The particles in angular soil interlocked causing the soil to act like a continuous area. This is because of the sharp corners in the particles and the higher friction. However, in rounded and

well-rounded materials, the soil particles can move more easily against each other. This caused movement and deformation under the footing. Changing the roundness of the soil particles affected the bearing capacity of the soil and the settlement of the footing. There was a decreased soil bearing capacity associated with the increasing roundness.

## 4 CONCLUSIONS

---

The soil behavior changes completely as a function of roundness. Both the particle shape and the roundness should be considered during engineering. This effect is more significant for finer materials. Beneath the affected layers of soil, angular particles are deeper than the rounded and well-rounded particles. These particles should be studied carefully. Angularity has an effect on the soil properties that change the soil's behavior at a distance of  $B$  ( $B$  is the footing width) from the footing edges. This affects the soil's behavior and should be studied in addition to the soils under the footing – even at a relative density of 30% for the angular soils. Increasing the roundness of the particles can affect the footing and the soil behavior because it depends strongly on the properties of the soil, especially under the footing. The larger relative densities of the angular soils with at least a depth of  $4B$  should be studied carefully, because even at this distance under the footing there is deformation and movement of the soil particles.

### Acknowledgment

We thank the Ataturk University and Geotechnical Engineering Division for providing us with the laboratory and equipment we needed for this study.

## REFERENCES

---

- [1] Santamrina, J. C., Cho, G. C. 2004. Soil behavior: the role of particle shape. In: *Advances in geotechnical engineering: the skempton conference*. 1, 604–617. DOI: 10.1680/aigev1.32644.0035
- [2] Cho, G. C., Dodds, J., Santamarina, J. C. 2006. Particle shape effects on packing density, stiffness, and strength: natural and crushed sands. *Journal of Geotechnical and Geoenvironmental Engineering* 132, 591–602. DOI:http://dx.doi.org/10.1061/(ASCE)1090-0241(2006)132:5(591)
- [3] Holtz, W. G., Gibbs, H. J. 1956. Triaxial shear tests on previous gravelly soils. *Journal of the Soil Mechanics and Foundations Division* 82(1), 1–22.
- [4] Cubrinovski, M., Ishihara, K. 2002. Maximum and minimum void ratio characteristics of sands. *Soils and Foundations* 42 (6), 65–78. DOI:http://doi.org/10.3208/sandf.42.6\_65
- [5] Arasan, S., Akbulut, S., Hasiloglu, A. S. 2010c. Effect of particle roundness on the maximum and minimum void ratios of granular soils. 13. National Soil Mechanics and Foundation Engineering Congress, (in Turkish with an English summary).
- [6] Yanrong, Li. 2013. Effects of particle shape and size distribution on the shear strength behavior of composite soils. *Bulletin of Engineering Geology and the Environment* 72, 371–381. DOI: 10.1007/s10064-013-0482-7
- [7] Arasan, S., Yener, E., Hattatoglu, F., Akbulut, S., Hinishlioglu, S. 2010d. The relationship between the fractal dimension and mechanical properties of asphalt Concrete. *International Journal of Civil and Structural Engineering* 1 (2), 165–170. DOI:10.6088/ijcser.00202010014.
- [8] Yang, F., Zheng, X. C., Zhao, L. H., Yi-Gao Tan 2016. Ultimate bearing capacity of a strip footing placed on sand with a rigid basement. *Computers and Geotechnics* 77, 115–119. DOI:10.1016/j.compgeo.2016.04.009
- [9] Choidhary, A. K., Jha, J. N., Gill, K. S. 2010. Laboratory investigation of Bearing Capacity Behavior of Strip Footing on Reinforced Fly Ash Slope. *Geotextiles and Geomembranes* 28, 393-402. DOI:10.1016/j.geotexmem.2009.09.007
- [10] Binquet, J., Lee, K.L. 1975a. Bearing capacity tests on reinforced earth slabs. *Journal of Geotechnical Engineering Division, ASCE* 101, 1241–1255.
- [11] Binquet, J., Lee, K.L. 1975b. Bearing capacity analysis of reinforced earth slabs. *Journal of Geotechnical Engineering Division, ASCE* 101, 1257–1276.
- [12] Akinmusuru, J.O., Akinbolade, J.A. 1981. Stability of loaded footings on reinforced soil. *Journal of Geotechnical Engineering Division, ASCE* 107, 819–827.
- [13] Das, B.M., Khing, K.H., Shin, E.C., Puri, V.K., Yen, S.C. 1994. Comparison of bearing capacity of strip foundation on geogrid-reinforced sand and clay. *Proceedings of the 8th International Conference on Computer Methods and Advances in Geomechanics, Morgantown, WA, USA* 1331–1336.
- [14] Fragaszy, R. J., Lawton, E. 1984. Bearing capacity of reinforced sand subgrades. *Journal of Geotechnical Engineering Division, ASCE* 110, 1501–1507.
- [15] Boiko, I. L., Alhassan, M. 2013. Effect of vertical cross-Sectional shape of foundation on settlement and bearing capacity of soils. *Procedia Engineering* 57, 207 – 212. DOI:10.1016/j.proeng.2013.04.029
- [16] El-Sawwaf, M., Nazir, A. K. 2010. Behavior of repeatedly loaded rectangular footing resting on reinforced sand. *Alexandria Engineering Journal* 49, 349–356. DOI:10.1016/j.aej.2010.07.002
- [17] Mostafa, A., El Sawwaf, M. 2007. Behavior of strip footing on geogrid-reinforced sand over soft clay slope. *Geotextiles and Geomembranes* 25, 50–60. DOI:10.1016/j.geotexmem.2006.06.001
- [18] Lee, J., Eun, J. 2009. Estimation of bearing capacity for multiple footing in sand. *Computer*

- and *Geotechnics Journal* 36 (6), 1000-1008.  
DOI:10.1016/j.compgeo.2009.03.009
- [19] Chen, Q., Abu-Farsakh, M. 2015. Ultimate bearing capacity analysis of strip footing on reinforced soil foundation. *Soils and Foundations* 55 (1), 74–85. DOI:10.1016/j.sandf.2014.12.006.
- [20] Kuranchie, F. A., Shukla, S. K., Habibi, D., Kazi, M. 2016. Load-Settlement behavior of a strip footing resting on iron ore tailing as a structural fill. *International Journal of Mining Science and Technology* 26, 247-253. DOI:10.1016/j.ijmst.2015.12.010
- [21] Cicek, E., Guler, E., Yetimoglu, T. 2015. Effect of reinforcement length for different geosynthetic reinforcement on strip footing on sand soil. *Soils and Foundations* 55 (4), 661–677. DOI:10.1016/j.sandf.2015.06.001
- [22] Cure, E., Turker, E., Uzuner, B, A. 2014. Analytical and experimental study for ultimate loads of eccentrically loaded model strip footings near a sand slope. *Ocean Engineering* 89, 113–118. DOI:10.1016/j.oceaneng.2014.07.018
- [23] Terzaghi, K. 1943. *Theoretical Soil Mechanics*. Wiley & Sons, New York.
- [24] Vesic, A. S., 1963. Bearing capacity of deep foundation in sand. *Highway Research Record*, National Academy of Science 39, 112-153.
- [25] Vesic, A. S. 1973. Analysis of ultimate loads of shallow foundations. *Journal of the soil mechanics and foundations division, American Society of civil engineers* 99 (1), 45-73.
- [26] Das, B. M. 2011. *Principles of Foundation Engineering*. Seventh Editions. Global Engineering. Christopher M. Shortt. Chapter 3, 133-134.
- [27] White, D.J., Take, W.A., Bolton, M.D. 2001. Measuring soil deformation in geotechnical models using digital images and PIV analysis. *International Conference on Computer Methods and Advances in Geomechanics* 997–1002.
- [28] White, D.J., Take, W.A., Bolton, M.D. 2003. Soil deformation measurement using particle image velocimetry (PIV) and photogrammetry. *Geotechnique* 53 (7), 619–631.
- [29] Slominski, C., Niedostatkiewicz, M., Tejchman, J. 2007. Application of particle image velocimetry (PIV) for deformation measurement during granular silo flow. *Powder Technology* 173 (1), 1-18. <http://dx.doi.org/10.1016/j.powtec.2006.11.018>
- [30] Ould Baba, H., Peth, S. 2012. Large scale soil box test to investigate soil deformation and creep movement on slopes by Particle Image Velocimetry (PIV). *Soil and Tillage Research* 125, 38-43. <http://dx.doi.org/10.1016/j.still.2012.05.021>
- [31] ASTM D 854-14, Standard Test Methods for Specific Gravity of Soil Solids by Water Pycnometer.
- [32] Arasan, S., Yener, E., Hattatoglu, F., Hinishioglu, S., Akbulut. S. 2010a. The correlation between shape of aggregate and mechanical properties of asphalt concrete: Digital image processing approach. *Road Materials and Pavement Design* 12 (2), 239–262. DOI:10.1080/14680629.2011.9695245
- [33] Cox, E. A. 1927. A method for assigning numerical and percentage values to the degree of roundness of sand grains. *Journal of Paleontology* 1 (3), 179–183.
- [34] Powers, M.C. 1953. A new roundness scale for sedimentary particles. *Journal of Sedimentary Petrology* 23, 117–119.
- [35] ASTM D 2487-11, Standard Practice for Classification of Soils for Engineering Purposes (Unified Soil Classification System).
- [36] ASTM D 6913-04, Standard Test Methods for Particle-Size Distribution (Gradation) of Soils Using Sieve Analysis.
- [37] ASTM D 4253 – 16, Standard Test Methods for Maximum Index Density and Unit Weight of Soils Using a Vibratory Table.
- [38] ASTM D 4254 – 16, Standard Test Methods for Minimum Index Density and Unit Weight of Soils and Calculation of Relative Density.
- [39] Arasan, S., Determination of some geotechnical properties of granular soils by image analysis, PhD Thesis, Ataturk University, Graduate school of natural and applied science, Department of civil engineering, (2011).